

An Integrated Active Filter Capabilities for Wind Energy Conversion Systems with Doubly Fed Induction Generator by Fuzzy

P. Bhaskara Prasad¹

Assistant Professor, Dept. EEE, A.I.T.S-Rajampet, A.P, India.

Dr. M. Padmalalitha²

Professor and H.O.D, Dept. EEE, A.I.T.S-Rajampet, A.P, India.

V. Sajjad Hyder³

PG Student, Dept. EEE, A.I.T.S-Rajampet, A.P, India.

Abstract

An integrated active filter Capabilities for wind energy conversion systems with Doubly fed induction generator using grid side converter (GSC) is presented in this paper. GSC converter is used for supplying harmonic in addition it transfer slip power. The main contribution of rotor side converter (RSC) is for attaining maximum power extraction and to supply reactive power to the DFIG. This wind energy conversion system (WECS) works as a static compensator (STATCOM) for supplying harmonics even it supply when the wind turbine is in shutdown condition. Control algorithms of both GSC and RSC are presented. Here fuzzy logic is used for controlling and the MATLAB/Simpower systems tool has proved that the power electronics tools and electrical elements tools are used for DFIG-based WECS for simulation.

Keywords: Doubly fed induction generator (DFIG), integrated active filter, nonlinear load, power quality, wind energy conversion system (WECS).

NOMENCLATURE

vab, vbc, vca	Three phase stator voltages.
isa, isb, isc	Three phase stator currents.
ira, irb, irc	Three phase rotor currents.
iga, igb, igc	Three phase grid currents.
ila, ilb, ilc	Three phase load currents.
igasca, igscb, igsc	Three phase grid-side convertor (GSC) currents.
Pg	Active power fed to the grid.
Qg	Reactive power fed to the grid.
Ps	Stator active power.
Qs	Stator reactive power.
Qs	Stator reactive power.
Pl	Load active power.
Ql	Load reactive power.
Pgsc	GSC active power.
Qgsc	GSC reactive power
v_w	Wind speed in m/s.
ω_r	Rotor speed in rad/s.
vdc	DC-link voltage.

I. INTRODUCTION

Now-a-days the electrical energy consumption is more due to increase in population & industrialization conventional energy sources such as coal, petrol, gas etc., are unlimited in nature. So we concentrate on renewable energy sources as solar energy, wind energy etc. The main advantage of the wind energy is ecofriendly and cost is free. In these days, wind turbines have been used as fixed speed wind turbines with squirrel cage induction generator and capacitor banks. Most of the wind turbines are fixed speed because of their simplicity and low cost. By observing the characteristics of the wind turbines it is clear that for getting maximum power, machine must rotate at variable rotor speed. So by using variable wind turbine system we can produce maximum amount of electrical energy. DFIG be the one of the most variable speed wind turbines are preferred because of low cost, higher energy output , lower converter rating.

The other uses of variable speed WECS such as power smoothening and harmonic mitigation and in addition to its power generation. Super magnetic energy storage systems are used for power smoothening. The other auxiliary requirement such as reactive power and transient stability limit are achieved including STATCOM.

A distribution STATCOM/(DSTATCOM) coupled with fly-wheel energy storage system is used at the wind farm for mitigating harmonics and frequency disturbances. Unified power quality conditioner (UPQC) is also used for improving power quality and reliability. Up to now separate converters are used for compensating the harmonics and also for controlling the reactive power. In a Single controller the harmonics compensation and reactive power control are achieved with the help of existing RSC. Therefore, harmonics are injected from the RSC into the rotor windings. This creates losses and noise in the machine. These methods increase the RSC rating. Now we are using GSC control for harmonic compensation and reactive power control. So harmonics cannot pass through the windings of the machine. RSC and GSC are needed for compensating the harmonics and controlling the reactive power.

Previously we are using direct current control of GSC. Therefore, harmonic compensation is not so effective and total harmonic distortion (THD) is not less than 5% as per IEEE-519 standard. An indirect current control technique is simple and shows enhanced performance for eliminating harmonics as compared to direct current control.

In this, a new control algorithm is proposed for GSC for compensating harmonics created by nonlinear loads and by using an indirect current control. RSC is used for the reactive power control of DFIG. The main advantage of proposed DFIG is work as an active filter even when the wind turbine is in blackout condition. Therefore, it compensates load reactive power and harmonics at wind turbine stalling case. By using Fuzzy the dynamic performance of the proposed DFIG is also demonstrated for varying wind speeds and also changes unbalanced nonlinear loads at point of common coupling (PCC).

II. SYSTEM CONFIGURATION AND OPERATING PRINCIPLE

Fig. 1 shows a schematic diagram of the proposed integrated active filter Capabilities for WECS with DFIG. In DFIG, the stator is directly connected to the grid as in Fig. 1. Two back-to-back connected voltage source converters (VSCs) are placed among the grid and rotor. Nonlinear loads are connected at PCC. DFIG can act as an active filter even when wind energy conversion system is in shutdown condition. The PCC voltage is distorted at the PCC point due to nonlinear loads. These non-linear load associated at the PCC voltage.

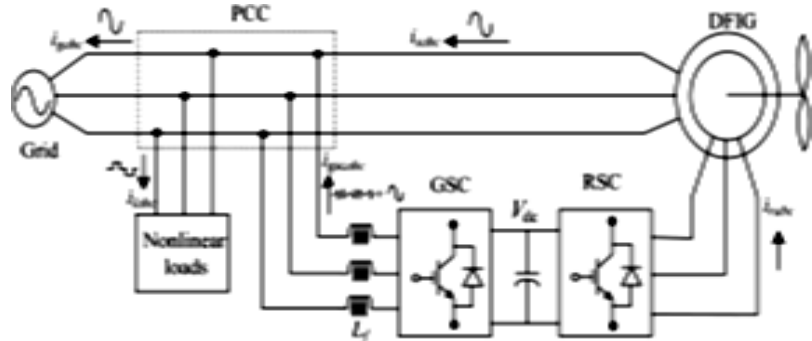


Fig. 1: Proposed system configuration.

These nonlinear load harmonic currents are mitigated by GSC control, so that the stator and grid currents are free from harmonics. RSC is controlled for achieving maximum power point tracking (MPPT) and also for unity power factor at the stator side using voltage-oriented reference frame. Synchronous reference frame (SRF) control method is used for extracting the fundamental component of load currents for the GSC control.

III. DESIGN OF DFIG-BASED WECS

For the successful operation of DFIG the selection of ratings for VSCs and dc-link voltage is very much important. In this section, a detailed design of VSCs and dc-link voltage is discussed for the simulation system used in the simpower systems.

A. Selection of DC-Link Voltage

Normally, the dc-link voltage of VSC must be greater than twice the peak of maximum phase voltage. The choice of dc link voltage depends on both rotor voltage and PCC voltage. While from the rotor side, the rotor voltage is slip times the stator voltage. DFIG used in this prototype has stator to rotor turns ratio as 2:1. Generally, the DFIG operating slip is ± 0.3 . So, the rotor voltage is always less than the PCC voltage. So, the design criteria for the selection of dc-link voltage can be achieved by considering only PCC voltage. Though considering from the GSC side, the PCC line voltage (v_{ab}) is 230 V, as the machine is connected in delta mode.

Therefore, the dc-link voltage is estimated as

$$v_{dc} \geq \frac{2\sqrt{2}}{\sqrt{3}*m} V_{ab} \quad (1)$$

where V_{ab} is the line voltage at the PCC. Maximum modulation key is selected as 1 for linear range. The value of dc-link voltage (V_{dc}) by (1) is valued as 375 V. Hence, it is nominated as 375 V.

B. Selection of VSC Rating

The DFIG pulls a lagging volt-ampere reactive (VAR) for its excitation to outline the rated air gap voltage. It is calculate from the machine parameters that the lagging VAR of 2 kVAR is needed when it is running as a motor. In DFIG situation, the operating speed range is 0.7 to 1.3 p.u. Therefore, the maximum slip (s_{max}) is 0.3. For making unity power factor at the stator side, reactive power of 600 VAR ($S_{max} * Q_s = 0.3 * 2 \text{ kVAR}$) is wanted from the rotor side (Q_{rmax}). The maximum rotor active power is ($S_{max} * P$). The power rating of the DFIG is 5 kW. Therefore, the maximum rotor active power (P_{rmax}) is 1.5 kW ($0.3 * 5 \text{ kW} = 1.5 \text{ kW}$).

So, the rating of the VSC as RSC S_{rated} is given as

$$S_{rated} = \sqrt{P_{rmax}^2 + Q_{rmax}^2} \quad (2)$$

Thus, kVA rating of RSC S_{rated} is intended as 1.615 kVA.

C. Design of Interfacing Inductor

The design of interfacing inductors between GSC and PCC be contingent upon allowable GSC current limit (i_{gscpp}), dc-link voltage, and switching frequency of GSC. Maximum conceivable GSC line currents are used for the calculation. Maximum line current depends upon the maximum power and the line voltage at GSC. The maximum conceivable power in the GSC is the slip power. In this case, the slip power is 1.5 kW. Line voltage (V_L) at the GSC is 230 V. So, the line current is obtained as $I_{gsc} = 1.5 \text{ kW}/(\sqrt{3} * 230) = 3.765 \text{ A}$. As the peak ripple current as 25% of valued GSC current, the inductor value is calculated as

$$L_i = \frac{\sqrt{3}mV_{dc}}{12af_m\Delta i_{gsc}} \quad (3)$$

Interfacing inductor between PCC and GSC is designated as 4 mH.

IV. CONTROL STRATEGY

Control algorithms for both GSC and RSC are shown in this control strategy. Complete control schematic is specified in Fig. 2. The control algorithm for emulating wind turbine features using dc machine and Type A chopper is also shown in Fig. 2.

A. Control of RSC

Mainly the RSC is to extract maximum power with independent control of active and reactive powers. The RSC is controlled in voltage-oriented reference edge. Therefore, the active and reactive powers are controlled by adjusting direct and quadrature axis rotor currents. Direct axis reference rotor current is nominated such that maximum power is extracted for a particular wind speed. Therefore, the outer loop is selected as a speed controller for achieving direct axis reference rotor current as

$$i_{dr}^*(k) = i_{dr}^*(k-1) + k_{pd}\{w_{er}(k) - w_{er}(k-1)\} + k_{id}w_{er}(k) \quad (4)$$

where the speed error (ω_{er}) is got by subtracting sensed speed (ω_r) from the reference speed (ω_*r). k_{pd} and k_{id} are the proportional and integral constants of the speed controller. $\omega_{er}(k)$ and $\omega_{er}(k-1)$ are the speed errors at k th and $(k-1)$ th instants. $i^{*dr}(k)$ and $i^{*dr}(k-1)$ are the direct axis rotor reference current at k th and $(k-1)$ th instants. Reference rotor speed (ω_*r) is estimated by optimal tip speed ratio control for a particular wind speed.

The correction of PI controllers used in both RSC and GSC are reached using Ziegler Nichols method. Initially, k_{id} value is set to zero and the value of k_{pd} was increased until the response stars oscillating with a period of T_i . Now, the value of k_{pd} is taken as $0.45 k_{pd}$ and k_{id} is taken as $1.2 k_{pd}/T_i$.

B. Control of GSC

The originality of this work lies in the control of this GSC for mitigating the harmonics formed by the nonlinear loads.

The control block diagram of GSC is shown in Fig. 2. Here, an indirect current control is applied on the grid currents for making them sinusoidal and balanced. Therefore, this GSC supplies the harmonics for making grid currents sinusoidal and balanced. These grid currents are designed by subtracting the load currents from the summation of stator currents and GSC currents. Active power component of GSC current is obtained by processing the dc-link voltage error (v_{dce}) between reference and estimated dc-link voltage (V_{dc}^* and V_{dc}) through PI controller as

$$i_{gsc}^*(k) = i_{gsc}^*(k-1) + k_{pd}v_{dce}(k)v_{dce}(k-1) + k_{id}v_{dce}(k) \quad (5)$$

where k_{pd} and k_{id} are proportional and integral improvements of dc-link voltage controller. $V_{dce}(k)$ and $V_{dce}(k-1)$ are dc link voltage faults at k th and $(k-1)$ th times. $i_{gsc}^*(k)$ and $i_{gsc}^*(k-1)$ are active power component of GSC current at k th and $(k-1)$ th instants.

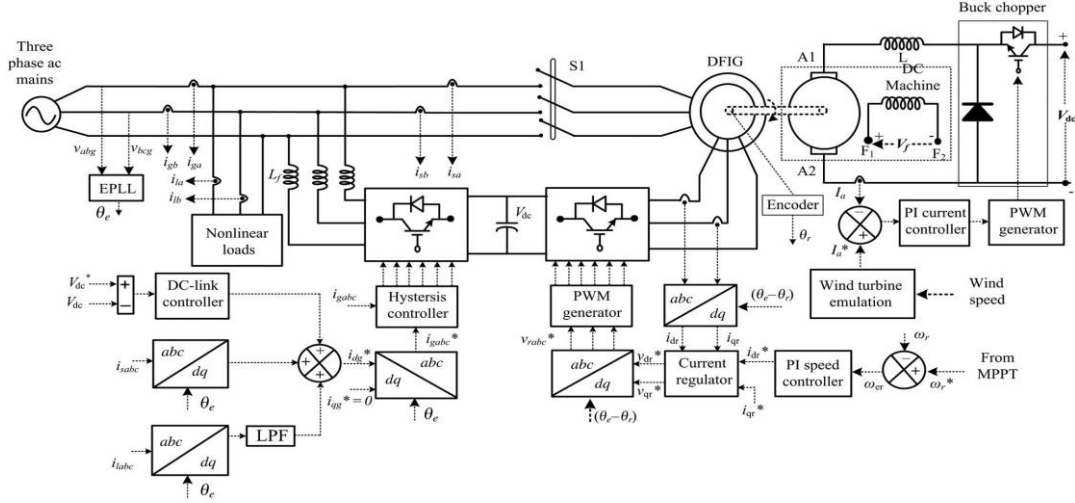


Fig. 2. Control algorithm of the proposed WECS.

V. FUZZY LOGIC CONTROLLER

In FLC, basic control act is resolute by a set of linguistic rules. These rules are determined by the system. Since the numerical variables are converted into linguistic variables, mathematical modeling of the system is not required in FC.

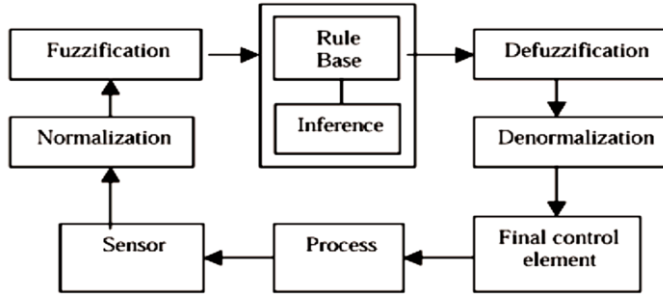


Fig. 3: Fuzzy logic Controller.

The FLC involves of three parts: fuzzification, interference engine and defuzzification. The FC is considered as i. fuzzy sets for every input and output. ii. Triangular membership functions for simplicity. iii. Fuzzification using continuous universe of address. iv. Implication using Mamdani's, 'min' operator. v. Defuzzification using the height method.

Fuzzification: Membership function principles are assigned to the linguistic variables, using seven fuzzy subsets: Negative Big, Positive Small, Positive Medium Negative Medium, Negative Small, Zero, and Positive Big. The Partition of fuzzy subsets and the shape of membership role adapt the shape up to appropriate system.

The value of input error and variation in error are normalized by an input mounting factor.

The input scaling factor has been designed such that input ethics are between -1 and +1. The triangular shape of the membership function of this arrangement presumes that for any particular $E(k)$ input there is only one main fuzzy subset. The input error for the FLC is given as

$$E(k) = \frac{P_{ph(k)} - P_{ph(k-1)}}{V_{ph(k)} - V_{ph(k-1)}} \quad (6)$$

$$CE(k) = E(k) - E(k-1) \quad (7)$$

Inference Method: Several composition methods such as Max-Dot and Max-Min have been planned in the literature. In this paper Min method is used. The output membership function of each rule is specified by the minimum operator and maximum operator.

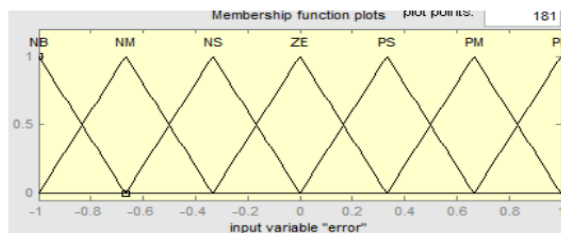


Fig.4: Membership functions

Defuzzification: As a plant usually requires a non-fuzzy value of control, a defuzzification period is wanted. To compute the output of the FLC, „height“ method is used and the FLC output modifies the control output. Further, the output of FLC controls the switch in the inverter. In UPQC, the active power, reactive power, terminal voltage of the line and capacitor voltage are required to be preserved. In order to control these parameters, they are sensed and compared with the reference values. To attain this, the membership functions of FC are: error, modification in error and output

The set of FC rules are derived from

$$u = -[\alpha E + (1-\alpha)*C] \quad (8)$$

Where α is self-adjustable factor which can adjust the whole operation. E is the error of the system, C is the change in error and u is the control variable. A large value of error E indicates that given system is not in the balanced state. If the scheme is unbalanced, the controller should enlarge its control variables to balance the system as

early as possible. On the other hand, small change of the error E indicates that the system is near to stable state.

VI. SIMULATION VALIDATION

By Fuzzy logic controller the simulated results are presented in this section for validating steady-state and dynamic performances of this DFIG with integrated active filter capabilities.

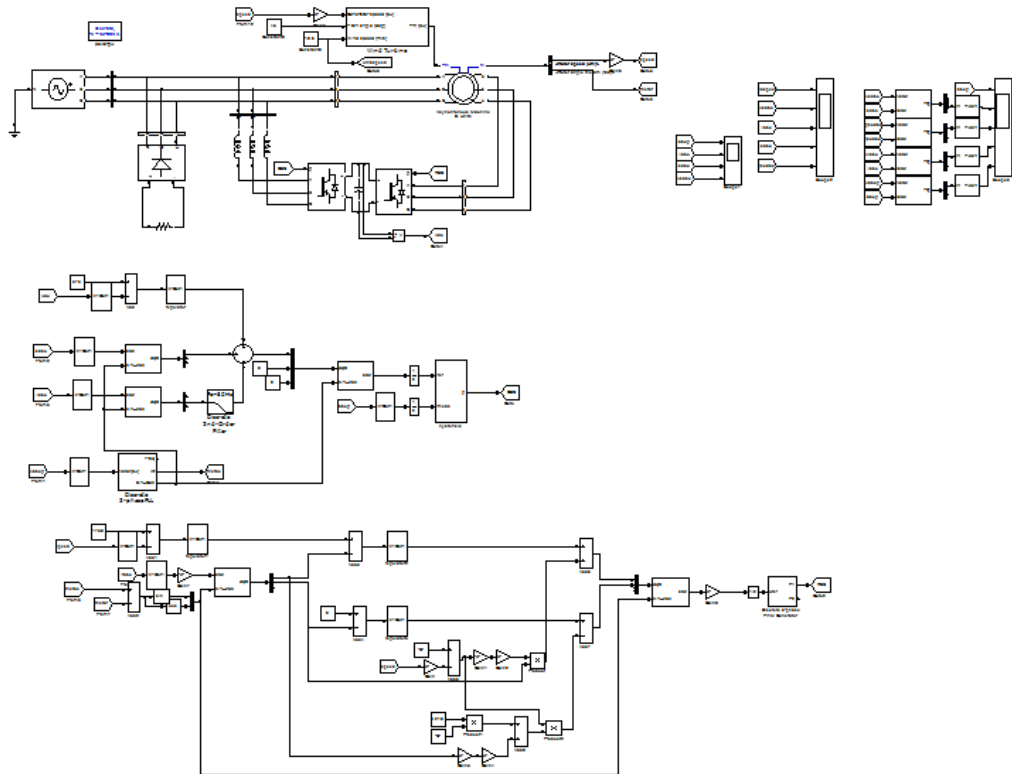


Fig. 5: Simulated Model

A. Steady-State Performance of DFIG-Based WECS with Integrated Active Filter Capabilities

The simulated performance of the DFIG is presented at a 10.6-m/s wind speed as shown in Fig. 6. The DFIG reference speed of the machine is taking as 1750 rpm when operating at MPPT. The load currents are nonlinear in nature. The GSC is supplying required harmonics currents to the load for making grid currents (i_{gabc}) and stator currents (i_{sabc}) balanced and sinusoidal. At above synchronous speed the power flow from GSC to PCC, so now the GSC power is become positive. The total power generated by the DFIF is sum of the stator power(P_s) and GSC power(P_{gsc}). The load power(P_l) is supplied then the remaining power is sent back to grid(P_g).

Fig. 7 shows the GSC working as an active filter even when the wind turbine is in stall condition. Here, stator currents are zero, as there is no power production from the DFIG then the load power is supplied from the grid. Therefore, the grid power (P_g) is observed to be negative. Now, this GSC supplies harmonic currents and reactive power. So, the reactive power taken from the grid (Q_g) is observed to be zero. Grid currents are observed to be balanced and sinusoidal even load currents are nonlinear.

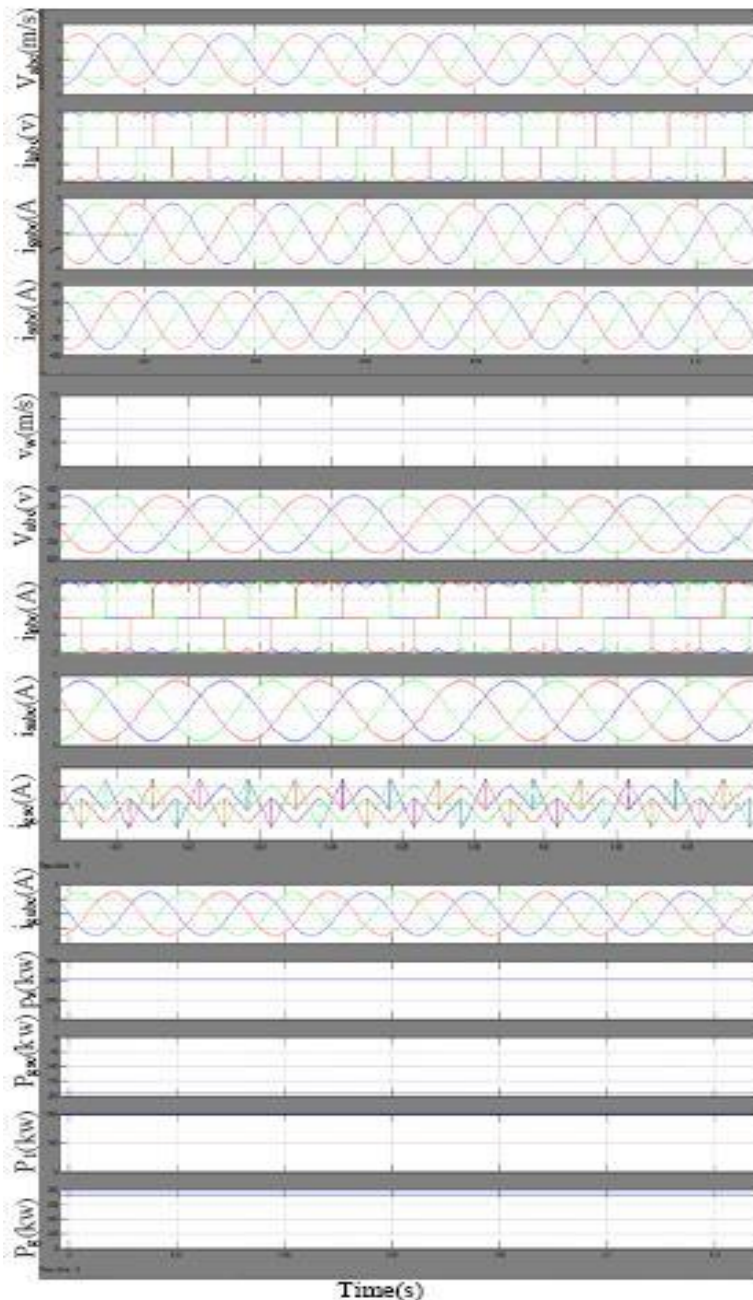


Fig. 6: Simulated performance of the proposed DFIG based W ECS at fixed wind speed of 10.6 m / s

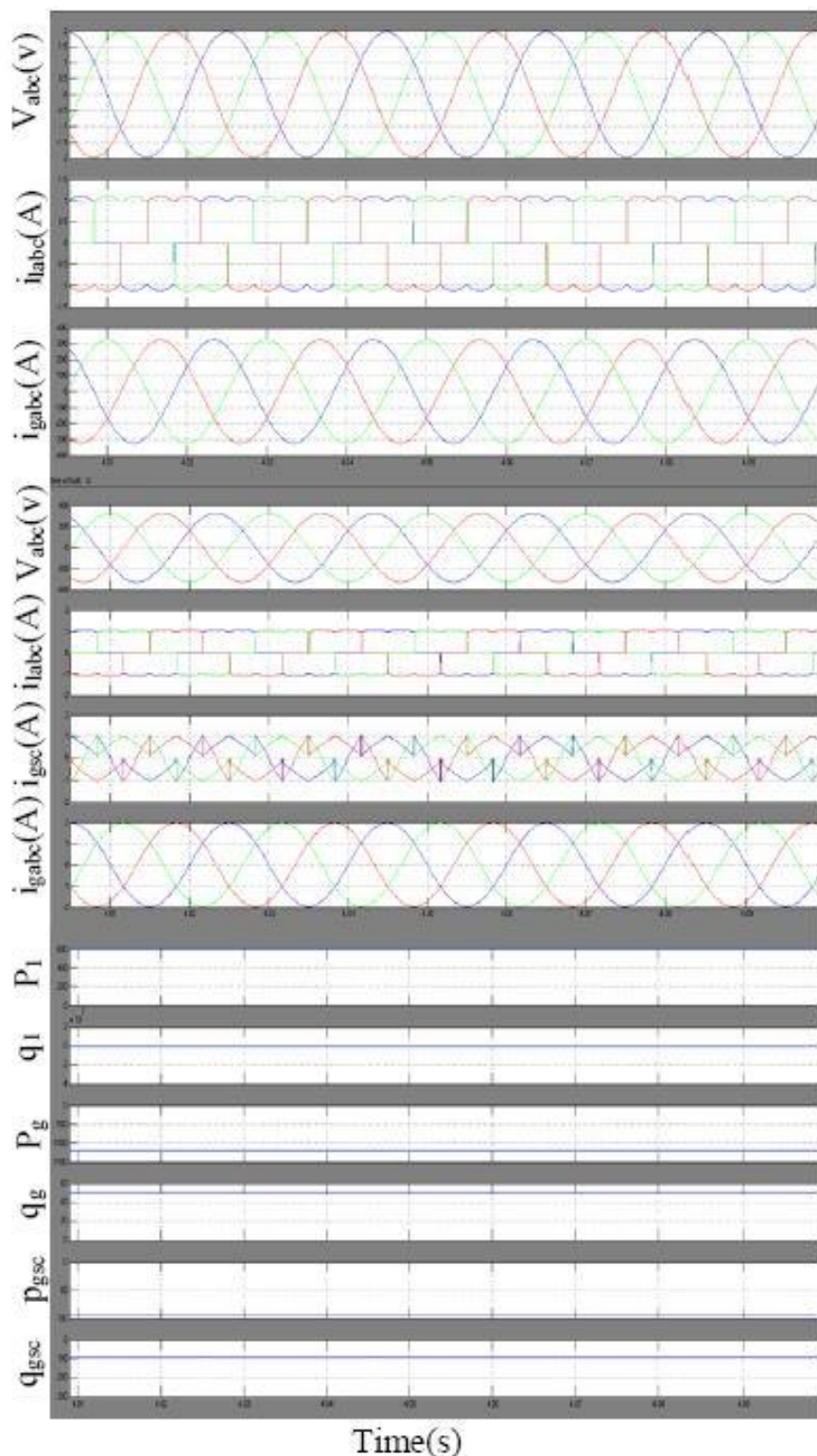


Fig. 7: Simulated performance of the proposed DFIG-based WECS working as a STATCOM at zero wind speed.

B. Dynamic Performance of DFIG-Based WECS with Integrated Active Filter Capabilities

Fig. 8 shows the simulation results for a decrease in wind speed. The reference speed (ω_{ref}) is decreased with the decrease in wind speed (v_w) for achieving MPPT operation. The actual rotor speed of the DFIG (ω_r) is also decreased with the reference speed. With the decrease in wind speed, the rotor speed (ω_r) of the DFIG is decreased from super synchronous speed to the sub synchronous speed and also the slip of the DFIG becomes positive from negative. Therefore, the power flow in the rotor is reversed. Previously, the rotor supplies power through GSC into the grid. As the speed reaches below synchronous speed, the rotor starts taking power from GSC into the rotor. Therefore, the GSC power is becoming negative.

The load power is taken as constant in this case. At high wind speeds, the excess power is feeding to the grid after supplying to the local load. As the wind speed decreases, the power generated by the DFIG is not sufficient to feed local loads. Therefore, the load is supplied from the grid. Therefore, the grid power(P_g) reverses its direction. As the speed changes from super synchronous speed to the sub synchronous speed, the change in the phase sequence of the rotor currents is observed.

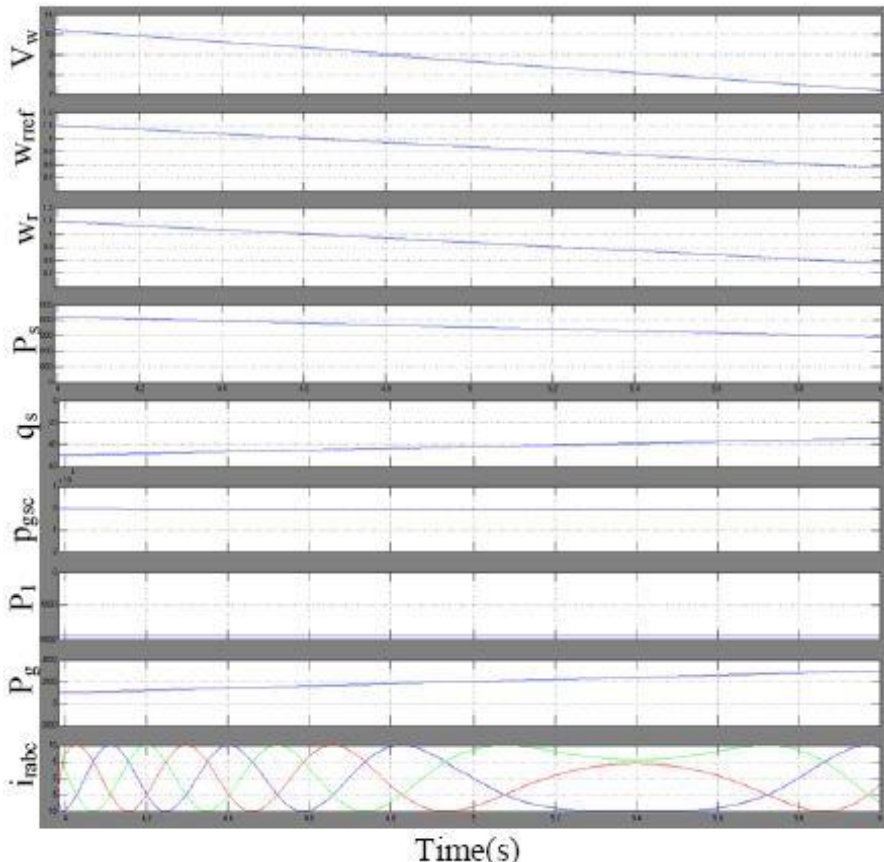


Fig.8: Simulated performance of proposed DFIG for fall in wind speed.

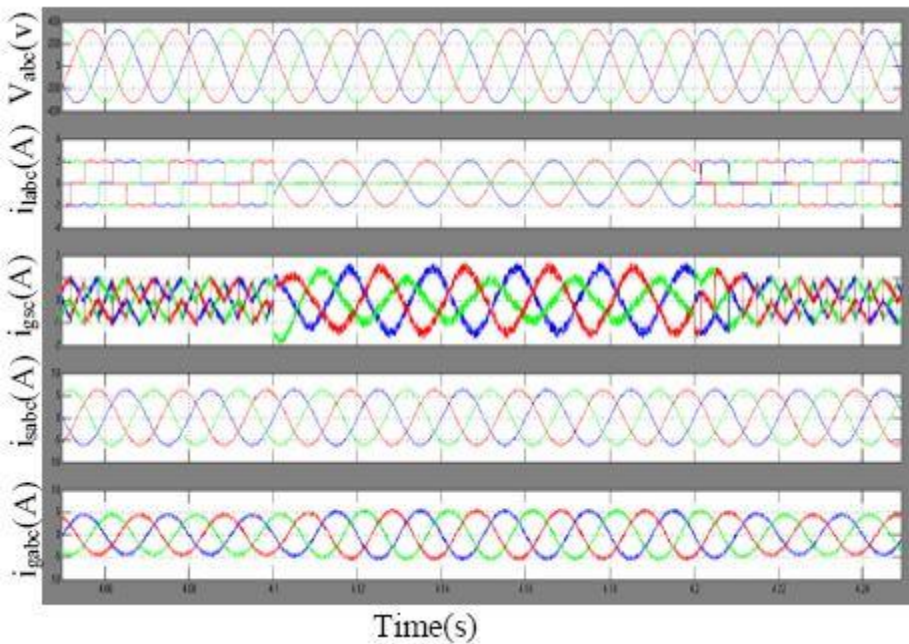


Fig.9: Dynamic performance of DFIG-based WECS for the sudden removal and application of local loads.

Fig. 9 shows the simulated performance for demonstrating the load compensation capability of the DFIG. This unbalanced load is emulated suddenly by removing one phase of a load. From the results, one can clearly observe that the stator and grid currents are observed to be balanced and sinusoidal even for the unbalanced load. Fig. 9 shows the dynamic performance of this DFIG-based WECS for the sudden removal and application of load on phase “a.” Even for the unbalanced or single phase loads, the stator and grid currents are balanced and sinusoidal by compensating the phase “a” current through GSC. GSC current (i_{gsc}) in phase “a” is increased suddenly for balancing grid currents. An increase in grid currents (i_{gabc}) is observed as net load decreases with removal of one phase.

V. CONCLUSION

The GSC control algorithm of the proposed DFIG has been modified for supplying the harmonics and reactive power of the local loads. The MATLAB/Simpower systems simulation shows sensible performances of this controller. When compared to alternative controllers here the Fuzzy Controller gives accurate performance. In this proposed DFIG, the reactive power for the induction machine has been supplied from the RSC and the load reactive power has been supplied from the GSC. The decoupled control of both active and reactive powers has been achieved by RSC control. The proposed DFIG has also been verified at wind turbine stalling condition for compensating harmonics and reactive power of local loads. This DFIG-based WECS with an integrated active filter has been simulated using MATLAB/Simulink

environment. Dynamic performance of this proposed GSC control algorithm has also been verified for the variation in the wind speeds and for local nonlinear load.

REFERENCES

- [1] D. M. Tagare, *Electric Power Generation the Changing Dimensions*. Piscataway, NJ, USA: IEEE Press, 2011.
- [2] G. M. Joselin Herbert, S. Iniyan, and D. Amutha, “A review of technical issues on the development of wind farms,” *Renew. Sustain. Energy Rev.*, vol. 32, pp. 619–641, 2014.
- [3] I. Munteanu, A. I. Bratu, N.-A. Cutululis, and E. Ceang, *Optimal Control of Wind Energy Systems Towards a Global Approach*. Berlin, Germany: Springer-Verlag, 2008.
- [4] A. A. B. Mohd Zin, H. A. Mahmoud Pesaran, A. B. Khairuddin, L. Jahanshaloo, and O. Shariati, “An overview on doubly fed induction generators controls and contributions to wind based electricity generation,” *Renew. Sustain. Energy Rev.*, vol. 27, pp. 692–708, Nov. 2013.
- [5] S. S. Murthy, B. Singh, P. K. Goel, and S. K. Tiwari, “A comparative study of fixed speed and variable speed wind energy conversion systems feeding the grid,” in *Proc. IEEE Conf. Power Electron. Drive Syst. (PEDS’07)*, Nov. 27–30, 2007, pp. 736–743.
- [6] D. S. Zinger and E. Muljadi, “Annualized wind energy improvement using variable speeds,” *IEEE Trans. Ind. Appl.*, vol. 33, no. 6, pp. 1444–1447, Nov./Dec. 1997.
- [7] H. Polinder, F. F. A. van der Pijl, G. J. de Vilder, and P. J. Tavner, “Comparison of direct-drive and geared generator concepts for wind turbines,” *IEEE Trans. Energy Convers.*, vol. 21, no. 3, pp. 725–733, Sep. 2006.
- [8] R. Datta and V. T. Ranganathan, “Variable-speed wind power generation using doubly fed wound rotor induction machine—A comparison with alternative schemes,” *IEEE Trans. Energy Convers.*, vol. 17, no. 3, pp. 414–421, Sep. 2002.
- [9] E. Muljadi, C. P. Butterfield, B. Parsons, and A. Ellis, “Effect of variable speed wind turbine generator on stability of a weak grid,” *IEEE Trans. Energy Convers.*, vol. 22, no. 1, pp. 29–36, Mar. 2007.
- [10] R. Pena, J. C. Clare, and G. M. Asher, “Doubly fed induction generator using back-to-back PWM converters and its application to variable-speed wind-energy generation,” *IEE Proc. Elect. Power Appl.*, vol. 143, no. 3, pp. 231–241, May 1996.
- [11] S. Muller, M. Deicke, and R. W. De Doncker, “Doubly fed induction generator systems for wind turbines,” *IEEE Ind. Appl. Mag.*, vol. 8, no. 3, pp. 26–33, May/Jun. 2002.
- [12] W. Qiao and R. G. Harley, “Grid connection requirements and solutions for DFIG wind turbines,” in *Proc. IEEE Energy 2030 Conf. (ENERGY’08)*, Nov. 7–18, 2008, pp. 1–8.

- [13] H. M. Hasanien, “A set-membership affine projection algorithm-based adaptive-controlled SMES units for wind farms output power smoothing,” *IEEE Trans. Sustain. Energy*, vol. 5, no. 4, pp. 1226–1233, Oct. 2014. [15] Z. Saad-Saoud, M. L. Lisboa, J. B. Ekanayake, N. Jenkins, and G. Strbac, “Application of STATCOMs to wind farms,” *IEE Proc. Gener. Transmiss. Distrib.*, vol. 145, no. 5, pp. 511–516, Sep. 1998.

AUTHOR'S PROFILE

V. SAJJAD HYDER : He was born in 1992. He obtained his Bachelor degree in Electrical and Electronics Engineering in 2013 from SVIST, Kadapa. Currently Pursuing his Post Graduation in Electrical Power Systems in AITS, Rajampet, Kadapa(dist.).

